ELSEVIER

Journal of Alloys and Compounds 408–412 (2006) 335–339

Journal of ALLOYS AND COMPOUNDS

www.elsevier.com/locate/jallcom

Effects of oblique deposition on magnetostrictive characteristics of $TbFe_2$ films formed by ion plating

Konosuke Muramatsu [a], Tomoko O. Yamaki, Noriyoshi Matsuoka [a], Mitsuaki Takeuchi [a], Yoshihito Matsumura [b,*], Hirohisa Uchida [b]

[a] Department of Applied Science, Graduate School of Engineering, Tokai University, 1117 Kitakaname, Hiratsuka, Kanagawa 259-1292 Japan
[b] Department of Applied Science, School of Engineering, Tokai University, 1117 Kitakaname, Hiratsuka, Kanagawa 259-1292 Japan

Abstract

The effects of oblique deposition to induce high magnetostrictive susceptibility and huge magnetostriction were studied. The giant magnetostrictive Tb–Fe films were prepared by an ion plating process with inclined vapor flux using substrates angled with 0, 30 and 60°. Increasing the substrate angle induced strongly in-plane magnetic anisotropy by the oblique deposition. The magnetic and magnetostrictive characteristics of Tb–Fe films were effected by an oblique anisotropy. The oblique anisotropy of Tb–Fe film may be induced by the shape anisotropy connected with columnar grain.

Keywords: Giant magnetostriction; Film; Tb–Fe; Oblique deposition

1. Introduction

The giant magnetostrictive (GM) materials exhibit huge magnetostriction over 1000 ppm [1]. The GM bulk compounds are applied to devices such as powerful sonars, linear actuators and oscillation dampers [2,3]. Recently, we reported the GM films prepared by several deposition processes such as vacuum flash evaporation [4–6], ion plating [7], magnetron sputtering [8] and ion beam sputtering processes [9,10]. The preparation conditions of $TbFe_2$ films such as partial pressures of residual gases, deposition rate, substrate temperature and deposition processes were found dominant factors to determine magnetostriction and magnetostrictive susceptibility at low magnetic field [4–6]. Remarkably, the ion plating (IP) is a most effective process for the GM film due to high energy flux and a high deposition rate and high adhesion of films to substrate [7]. However the $TbFe_2$ film shows low magnetostriction at low applied fields corresponding to its perpendicular anisotropy.

A unique structure and properties of oblique deposited films have been extensively investigated since the end of the 1950’s [11]. These properties of oblique deposited films have controlled, and applied to industry, for example, magnetic recording tapes [12] and film for optical retardation plate [13]. Oblique deposition is expected to improve magnetostrictive susceptibility because in-plane anisotropy of magnetization is enhanced by magnetic shape anisotropy of columnar grains inclined in plane [14,15]. In this study, preparation of the giant magnetostrictive Tb–Fe films by the IP process was investigated to induce high magnetostrictive susceptibility and high magnetostriction at low applied magnetic fields, especially in respect to the effects of incidence of the vapor flux by geometrical arrangement of the tilted substrate.

2. Experimental

2.1. Ion plating system

Fig. 1 shows the schematic diagram of the IP system. This process produces variety of film character. Because dense plasma flux (∼2.5A) of a source material can be dosed and

---

[*] Corresponding author. Tel.: +81 463 58 1211x4909;
fax: +81 463 58 9461.
E-mail address: ncc1701d@keyaki.cc.u-tokai.ac.jp (Y. Matsumura).

0925-8388/$ – see front matter © 2005 Elsevier B.V. All rights reserved.
doi:10.1016/j.jallcom.2005.04.077

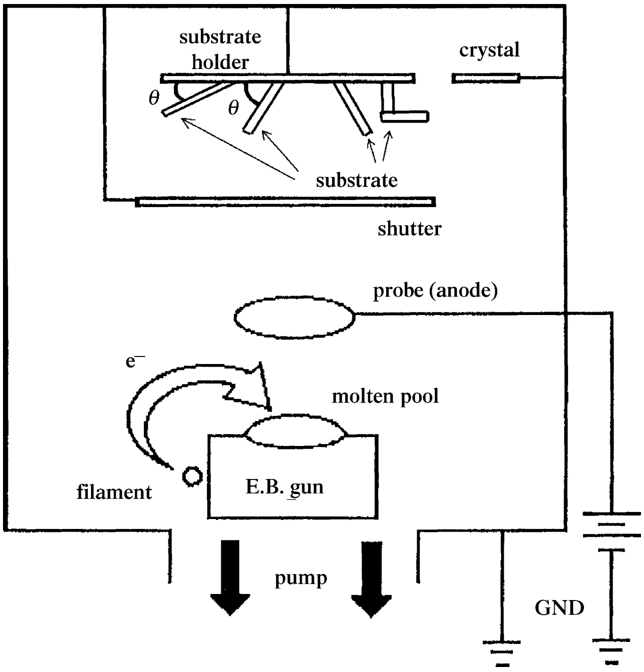

Fig. 1. Schematic diagram of IP system.

deposited on a substrate. The flux of the source material evaporated by an electron beam is activated by thermal electrons accelerated between a surface of the source and a probe. To achieve oblique deposition, several substrates were fixed to substrate holders with several angles from $\theta = 0°$ to 60° as shown in Fig. 2.

2.2. Film preparation

Bulk Tb–Fe alloy samples for evaporation were prepared by arc melting of Tb and Tb–Fe eutectic alloy (the purity of each element was 99.9%) in an Ar gas atmosphere. A composition of the film samples were dependent on the evaporant composition, a $TbFe_2$ film sample was obtained from a $Tb_{50}Fe_{50}$ evaporant resulted from energy dispersive X-ray spectroscopy. Table 1 shows a deposition condition of the film formed by IP process. We measured substrate temperature with thermocouple was established near the substrate. Substrate temperature was almost kept definite temperature.

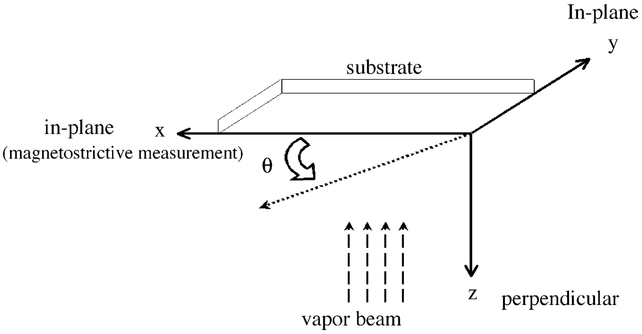

Fig. 2. Schematic representation of oblique deposition and directions of substrate angle.

Table 1
Condition of the formation by IP process

Base pressure (Pa)	5.5×10^{-5} to 1.0×10^{-4}
Deposition rate (nm/s)	4–10
Substrate temperature (K)	400
Deposit time (s)	120–180
Film thickness (m)	1.2–0.5
Anode potential (V)	100
Discharge current (A)	2.0–2.5
Substrate angle (°)	0, 30, 60
Substrate	Si (1 0 0)
Leak rate (Pa/s)	3.32×10^{-6}

2.3. Sample analysis

Morphology observations of fracture cross section of the film samples were used by scanning electron microscope (SEM). The composition of the film samples was determined using energy dispersive X-ray spectroscopy (EDX). The film structures were analyzed by X-ray diffraction (XRD) (Cu Kα) and transmission electron microscope (TEM). The magnetization of formed film samples was measured as a function of magnetic field using vibrating sample magnetometer (VSM) in the range from −15kOe to +15kOe. In magnetization measurements, directions of sample measurement were x, y, and z axes (in Fig. 2). The magnetostriction of the films along with x axes was measured by using a cantilever method described elsewhere [2]. The equation of the magnetostriction is as follows [16]:

$$\Delta\lambda_{//} = \frac{d t_s^2 E_s (1 + \nu_f)}{3 t_f l^2 E_f (1 - n_s)}.$$

where $E_f = 76$G-Young modulus Poisson's ratio of Tb–Fe_2 film [pa]; $\nu_f = 0.4$-Poisson's ratio of Tb–Fe_2 film; $E_s = 130$G-Young modulus Poisson's ratio of Si (1 0 0) substrate [pa]; $\nu_s = 0.28$-Poisson's ratio of Si (1 0 0) substrate [17].

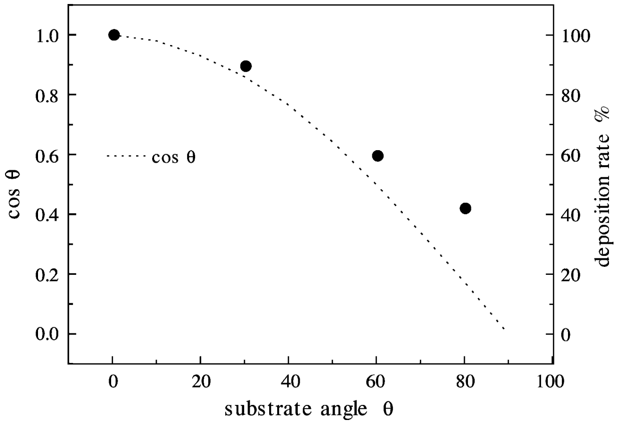

Fig. 3. Deposition rate of the films prepared by IP process under different substrate angles.

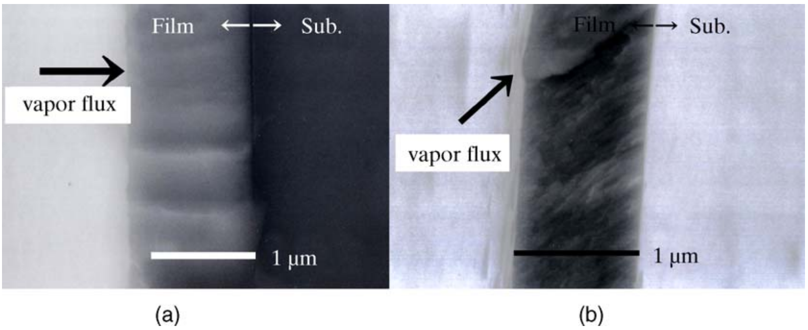

Fig. 4. SEM images of the films (fracture cross section): (a) substrate angle $\theta = 0^\circ$ and (b) substrate angle $\theta = 60^\circ$.

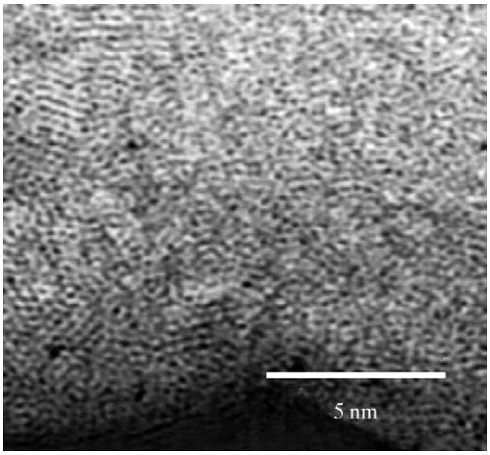

Fig. 5. TEM images of the film sample by IP process at room temperature.

3. Result and discussion

3.1. Deposition rate

Fig. 3 shows dependence of the deposition angles to deposition rate of the films. Increasing substrate angle caused the films thin because increasing substrate angle leads to increase shadow area. However, the larger the angle θ increased, the more ratio of deposition rate disagreed with random cosine distribution.

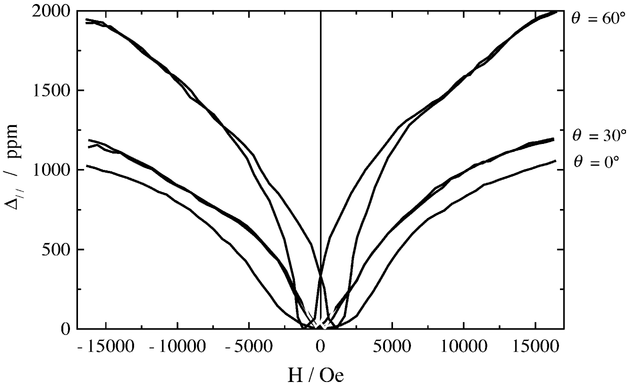

Fig. 6. Magnetostriction of film samples prepared by IP process under different substrate angles.

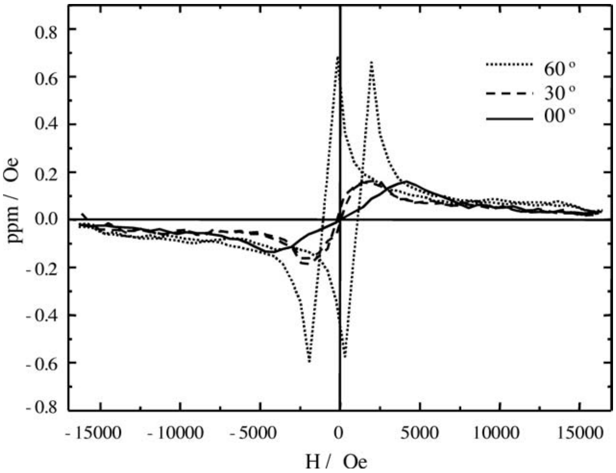

Fig. 7. Magnetostrictive susceptibility of film samples prepared by IP process under different substrate angles.

3.2. Morphology of the film

Fig. 4 shows the SEM fracture cross section micrographs of the films prepared by a deposition normal to substrate at $\theta = 0^\circ$ (Fig. 4(a)) and by an oblique deposition at $\theta = 60^\circ$

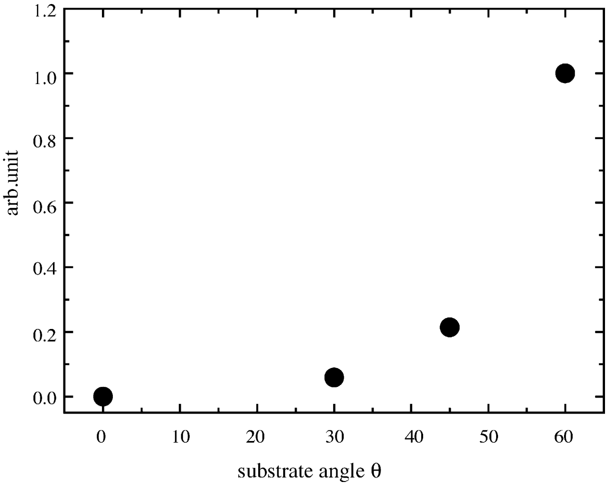

Fig. 8. A relative magnetostrictive hysteresis defined as area surrounded by magnetostrictive curves.

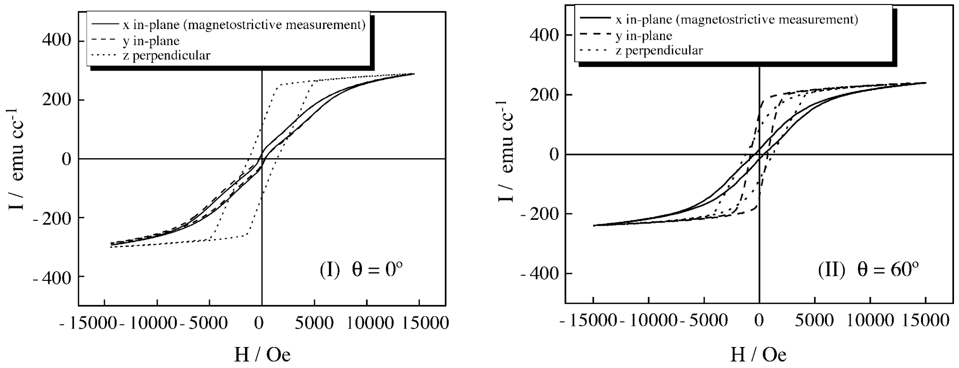

Fig. 9. Magnetization curves of films prepared by IP process under different substrate angles: (I) $\theta = 0°$ and (II) $\theta = 60°$.

(Fig. 4(b)). Columnar grains were found to grow in the direction of the incident vapor flux. When the vapor flux is oblique incident, atoms in the growing films shadow unoccupied sites from the direct sticking of incidence atoms. Moreover, owing to limited mobility, the unoccupied sites are not filled. This supports the result of film thickness as shown in Fig. 3. As a result, oblique columns grew in the direction of the incident vapor flux.

3.3. Crystal structure of the film

XRD result showed no distinct diffraction peak was observed for each sample. In previous work, we found that the crystal structure of thin film samples was found dependent on deposition conditions such as deposition rates and substrate temperatures [7]. In this study, the substrate temperature was from 293 to 333 K, and the deposition rate was 10 nm/s. The crystal structure of film samples by oblique deposition was independent of incidence angles.

Fig. 5 shows a TEM image of the $TbFe_2$ film sample prepared by IP process at room temperature. An amorphous phase was found to coexist with a nanocrystalline phase (<5 nm). Therefore the SEM and TEM observations and XRD analyses suggest that the $TbFe_2$ films were composed of columnar grains with amorphous and nanocrystalline phases.

3.4. Magnetostrictive properties

Fig. 6 shows a dependence of the deposition angles to magnetostriction. The film sample with 60° showed a higher magnetostrictive susceptibility and larger magnestostriction at low magnetic fields than the sample deposited normal to the substrate ($\theta = 0°$).

Fig. 7 shows magnetostrictive susceptibility of the film samples prepared by the IP process under different substrate angles. The magnetostrictive susceptibility increased with increasing substrate angle. The 60° film sample exhibited magnetostrictive susceptibility of 7 ppm/Oe. Oblique deposition is effective to improve magnetostrictive susceptibility.

Fig. 8 shows a dependence of the deposition angles to an area of magnetostrictive hysteresis. A relative magnetostrictive hysteresis is defined as area surrounded by magnetostrictive curves. The 60° film sample exhibited hysteresis in magnetostriction while almost no hysteresis was measured for the sample prepared at $\theta = 0°$. In our previous study, we described that the occlusion of contaminative gas atoms yields hysteresis effect [6]. In addition, more contaminative gas atoms can be occluded by an oblique deposition [11]. Our previous study of the formation of Tb–Fe films by the IP process showed magnetostriction without hysteresis [7]. Comparing with that study, our present study was made under a vacuum of $3.0–6.0 \times 10^{-4}$ Pa, which is lower than the vacuum of $2.9–5.0 \times 10^{-5}$ Pa of ref. [7]. This slightly inferior condition may cause the hysteresis effect.

3.5. Magnetic properties

Fig. 9 shows the magnetization curves of films prepared by IP process under different substrate angles, $\theta = 0°$, $\theta = 60°$. By TEM and XRD observations, the microstructure of samples exhibited the coexistence of amorphous and nanocrystalline (below 5 nm) phases. The 0° film exhibited perpendicular anisotropic magnetization. This result is in good agreement with results of our previous study [7] that magnetic films prepared by IP process tend to exhibit perpendicular anisotropic magnetization because of the induction of high internal stresses inside the film by a high deposition rate and high adhesion of films to substrate.

With increasing substrate angle, the saturated magnetization decreased from 290 to 240 emu/cc. This result was caused by decrease of film density due to shadow effect corresponding to Figs. 3 and 5. The high magnetic susceptibility by oblique deposition improved the magnetostriction at low magnetic fields.

4. Conclusion

Magnetic properties of oblique deposited $TbFe_2$ films prepared by IP process were investigated. The oblique deposition produced a columnar structure where each column was found composed of a mixture of amorphous and nanocrystalline phases. Magnetic properties of the film prepared by IP process were found to depend upon shape magnetic anisotropy, i.e. columnar grain morphology. The oblique deposition by IP process is effective for preparation of giant magnetostrictive films to induce high magnetostrictive susceptibility and high magnetostriction.

Acknowledgement

We are thankful to Tokyo Ohka Foundation for the Promotion of Science and Technology for financial support of this work.

References

[1] A.E. Clark, E.P. Wohlfahrt, Ferromagnetic Materials, vol. 1, North Holland, Amsterdam, 1980, Chapter 7.

[2] V. Koeninger, Y. Matsumura, T. Noguchi, H.H. Uchida, H. Uchida, H. Funakura, H. Kaneko, T. Kuroki, Proceedings of the International Symposium on Giant Magnetostrictive Materials and their Applications, 1992, pp. 151–156.

[3] H. Uchida, M. Wada, A. Ichikawa, Y. Matsumuta, H.H. Uchida, Proceedings of the Fifth International Conference On New Actuators, ACTUATOR'96, 1996, pp. 275–278.

[4] M. Wada, H. Uchida, H. Kaneko, J. Alloys Compd. 258 (1997) 143–147.

[5] M. Wada, H. Uchida, H. Kaneko, J. Alloys Compd. 258 (1997) 169–173.

[6] M. Wada, H.H. Uchida, H. Uchida, J. Alloys Compd. 258 (1997) 174–178.

[7] Y. Matsumura, H. Uchida, M. Ono, H. Kaneko, Proc. of the 16th Int. Workshop on Rare-Earth Magnets and their Applications, The Japan Institute of Metals, Sendai, 2000, pp. 985–994.

[8] K. Nakazato, M. Hashimoto, H. Uchida, Y. Matsumura, Rev. Sci. Instrum. 71 (2000) 996–1001.

[9] M. Wada, H.H. Uchida, Y. Matsumuta, H. Uchida, H. Kaneko, Thin Solid Films 281–282 (1996) 503–506.

[10] H.H. Uchida, V. Koeninger, H. Kaneko, J. Alloys Compd. 211–212 (1994) 455–459.

[11] R. Messier, A. Lakhtakia, Mater. Res. Innovations 2 (1999) 217.

[12] E. Kita, M. Kamikubota, A. Tasaki, K. Tagawa, IEEE Trans. Magn. 17 (6) (1981) 3193–3195.

[13] T. Motohiro, Y. Taga, Appl. Optics 28 (13) (1989) 2466–2482.

[14] T. Otiti, J. Mater. Sci. 39 (2) (2004) 477–480.

[15] H.-M. Ho, G. Thomas, J. Appl. Phys. 65 (8) (1989) 3161–3166.

[16] A.C. Tam, H. Schroeder, IEEE Trans. Magn. 25 (1989) 2629.

[17] J.J. Wortman, R.A. Evans, J. Appl. Phys. 36 (1965) 153.